Impact of carbon nanotubes on grain growth during spark plasma sintering of a 3YSZ matrix composite with statistical analysis

Alexander M. Laptev [a *], Wiktoria Krzyżaniak [a], Maria Wiśniewska [a], Martin Bram [b], Doris Sebold [b], Dariusz Garbiec [a]

[a] *Łukasiewicz Research Network – Poznań Institute of Technology, 6 Ewarysta Estkowskiego St., 61-755 Poznań, Poland*

[b] *Institute of Energy Materials and Devices – Materials Synthesis and Processing, Forschungszentrum Jülich GmbH, 52425 Jülich, Germany*

[*] Corresponding author.

E-mail address: alexander.laptev@pit.lukasiewicz.gov.pl (A.M. Laptev)

Keywords:

(A) Hot pressing

(A) Grain growth

(B) Grain size

(D) ZrO_2

Abstract

Carbon nanotubes (CNTs) are widely recognized as reinforcements in ceramic matrix composites (CMCs). Many studies highlight the effect of CNTs on the mechanical properties and other characteristics of CMCs. However, only a few articles explore the impact of CNTs on the microstructure of the ceramic matrix. This article investigates grain growth in zirconia (3YSZ) reinforced with 10 vol. % multi-walled carbon nanotubes (MWCNT) during spark plasma sintering (SPS) at a temperature of 1350°C. The grain size was evaluated using image processing and statistical analysis. MWCNTs moderately influence the grain size in the 3YSZ-10MWCNT composite sintered at 1350°C. The grain size in the MWCNT-rich region of the composite is 1.6 to 1.7 times smaller than that in the residual 3YSZ agglomerates and 2.0 to 2.2 times smaller than in 3YSZ samples without MWCNTs. The reduced grain growth results from the pinning of zirconia grain boundaries at the incoherent 3YSZ/MWCNT interface. The literature refers to this

phenomenon as Zener pinning. Additionally, individual MWCNTs and MWCNT agglomerates hinder grain fusion. Lastly, the reaction between carbon and zirconia can lead to the formation of oxycarbide (ZrOxCy) precipitates, which hinder grain growth through the Zener effect. The SPS sintering at 1350°C resulted in full densification of the 3YSZ samples with an HV1 hardness of 13.2 to 14.5 GPa. The residual porosity of the 3YSZ-10MWCNT samples was approximately 3.5%, while the HV1 hardness was around 7.6 GPa. The hardness values align with the typical ones for 3YSZ ceramics and the 3YSZ-10MWCNT composite.

1. Introduction

Carbon nanotubes are a fiber-like allotropy of carbon frequently used as reinforcement (filler) in various composites [**1**]. The literature distinguishes single-wall, double-wall, and multi-wall carbon nanotubes (SWCNT, DWCNT, MWCNT) according to their structure [**2**]. Many articles consider CNT-reinforced ceramic matrix composites, their synthesis, properties, and application, including composites with zirconia matrix [**2–5**]. The last CMC group typically has a 3YSZ matrix (zirconia partially stabilized with 3 mol % Y_2O_3) with improved crack resistance [**6–8**]. The CNT filler increases the fracture toughness and electrical conductivity but usually decreases the hardness, flexural strength, and thermal conductivity of 3YSZ-CNT composites [**9–12**]. Techniques used to synthase dense 3YSZ-CNT composites include spark plasma sintering [**10–13**] or hot pressing [**7,14**] at temperatures of 1200–1350°C and above.

When sintering at elevated temperatures, carbon nanotubes interact with the zirconia matrix. Maitre and Lefort investigated the reaction between carbon and zirconia [**15**]. This and other works report the formation of oxycarbide (ZrO_xC_y) at 1350-1600°C with an amount depending on temperature and holding time [**15,16**]. Giorgi et al. studied the formation of ZrC_x and ZrO_xC_y during SPS of a mixture of undoped ZrO_2 and carbon black [**17**]. The article reports onset temperatures of 1300°C during pressureless sintering and 1800°C when sintering at 16 MPa.

The presence of CNTs can influence grain growth in the 3YSZ matrix. Milsom et al. studied grain growth in the 3YSZ-MWCNT composite during SPS at 1500–1800°C. The authors noticed a significant decrease in grain size in sintered 3YSZ-MWCNT composites compared to 3YSZ ceramics [**18**]. The paper highlights the growing influence of carbon nanotubes on grain size as the content of MWCNT increases. Another paper published by this group reports the onset of this effect already at a temperature of 1350°C [**19**]. Furthermore, Mazaheri et al. observed decreased grain growth in 3YSZ-MWCNT composites after SPS at 1250°C [**6**]. Karanam et al. noticed an influence of CNTs on grain size after sintering 8YSZ-MWCNT composites at 1300°C [**20**]. Some authors explain the impeding effect of CNTs on grain growth in zirconia by poor wettability of the

ceramic matrix [**18**], the formation of a CNT network around the grains [**21**], and grain boundary pinning [**22**].

In our earlier work on the SPS of the 3YSZ-10MWCNT composite, we observed a notable difference between grain size in the residual 3YSZ agglomerates and areas containing MWCNT reinforcement [**23**]. This feature is investigated in detail in the present paper. The article compares the grain size in three sintered samples. The first sample was SPS sintered from the initially agglomerated 3YSZ powder supplied by the manufacturer. The second sample was sintered from the same powder and sonicated to disintegrate the 3YSZ agglomerates. The third sample was manufactured from the 3YSZ-10MWCNT mixture. The samples are denoted in this article as 3YSZ_aggl, 3YSZ_son, and 3YSZ-10MWCNT. The influence of powder sonication and MWCNTs on grain growth was investigated through statistical analysis of microstructure. The study of the 3YSZ-10MWCNT sample revealed the notable difference between grain size in residual 3YSZ agglomerates and areas with MWCNTs dispersed in the 3YSZ matrix. The residual 3YSZ agglomerates in the 3YSZ-10MWCNT composites allow a direct study of the MWCNT's impact on grain size within a single sample. The grain size evaluation was performed using image processing and statistical analysis. This approach is more informative than conventional grain size averaging. The paper explains the effect of carbon nanotubes on decreasing grain growth in zirconia by pinning grain boundaries with MWCNTs and ZrO_xC_y precipitations (Zener pinning) and preventing grain fusion.

2. Experimental

2.1. Powders and mixture

The matrix material was the partially stabilized 3YSZ powder (grade TZ-3Y-E) delivered by Tosoh (Japan). The 3YSZ powder consisted of primary particles with a size of around 40 nm merged into spherical agglomerates with a diameter of 20-200 μm **(Figs. 1a and 1b**). Multi-walled carbon nanotubes (NC7000 series) were supplied by Nanocyl SA (Belgium). The 3YSZ powder was sonicated for 3 min in isopropyl alcohol using a Sonic 14 bath (Polsonic, Poland). The short sonication time enabled the preservation of a certain number of 3YSZ agglomerates (**Fig. 1c**). The suspension was dried in a CLN32STD laboratory incubator (Pol-Eko-Aparatura, Poland) at 60°C for 48 hours. The dried powder was crushed in an agate mortar. The powder was used to sinter the 3YSZ_son sample.

Fig. 2 shows the particle size distributions (PSD) for the starting and sonicated 3YSZ powders studied with a Mastersizer 3000 (Malvern Panalytical, UK) laser diffraction analyzer according to

ISO 13320:2020. The powders were dispersed in distilled water and flashed by light sources with wavelengths 470 and 632.8 nm. Light scattering results were analyzed using Mie theory with a 3YSZ refraction index of 2.148. The imaginary part of the refraction index was set to 1 [**24**]. The results in **Fig. 2** illustrate the presence of residual 3YSZ agglomerates after sonication.

The preparation of the 3YSZ-10MWCNT mixture is described in detail elsewhere [**23**]. The MWCNTs were sonicated for 30 minutes. Then, the ball-milled 3YSZ powder was added, and the ultrasonic dispersion continued for another 30 min. The resulting mixture included primary 3YSZ particles, MWCNTs, and 3YSZ agglomerates (**Fig. 1d**).

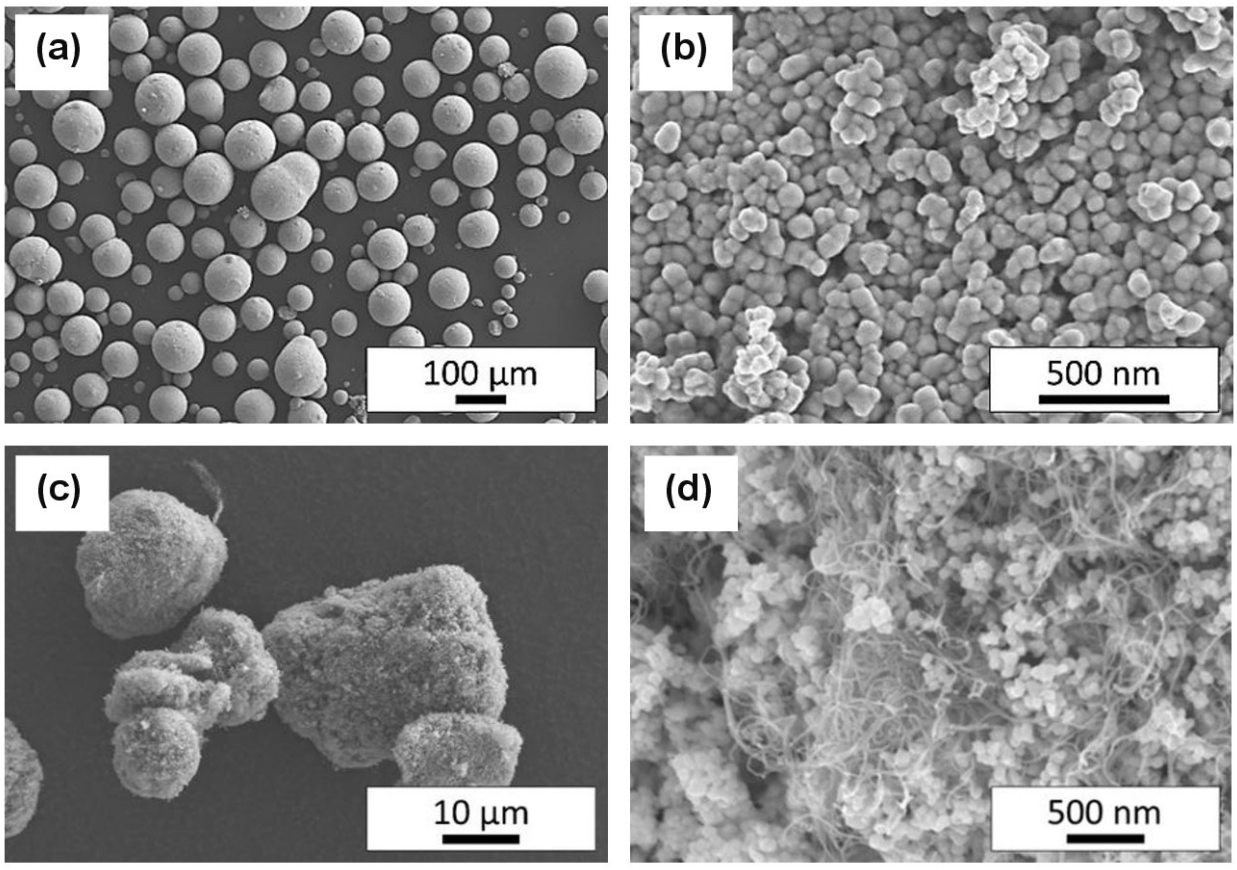

Fig. 1. (a) Initial 3YSZ agglomerates and (b) primary 3YSZ particles. (c) Loose 3YSZ agglomerates after sonication and (d) the 3YSZ-10MWCNT mixture.

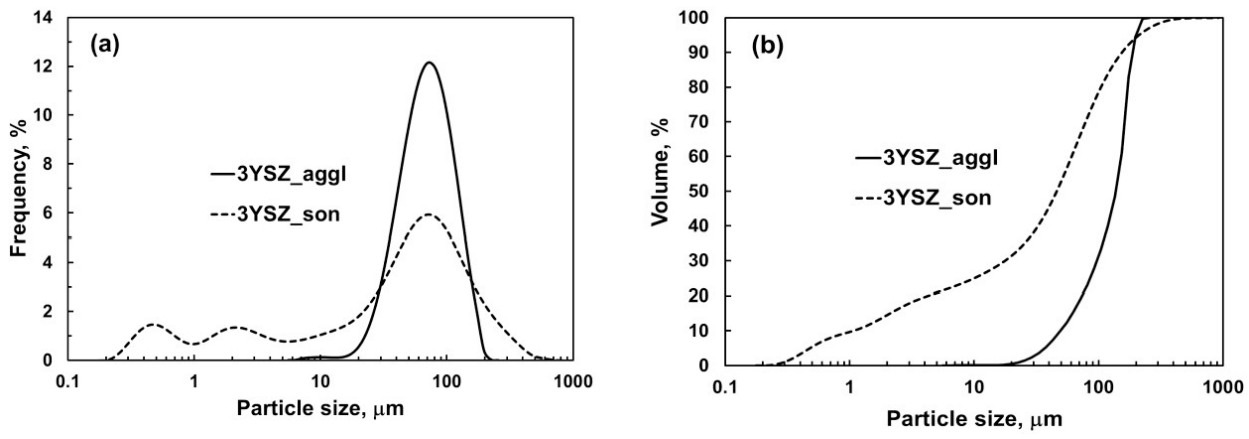

Fig. 2. (a) Differential and (b) cumulative particle size distributions for initial and sonicated 3YSZ powders.

2.2. Sintering

All samples were sintered at 1350°C under a vacuum of about 0.05 mbar in an HP D 25/3 SPS furnace (FCT Systeme, Germany). This temperature ensures the nearly full densification of the 3YSZ-10MWCNT composite with moderate grain growth in the 3YSZ matrix. The tooling was adapted to the design of this furnace [**25**]. In particular, the temperature was measured near the top of the sample using a pyrometer. The graphite die (2334 Mersen, France) was thermally insulated with 10 mm thick graphite felt (SGL Carbon, Germany) to reduce the thermal gradient in the sample [**26**]. **Table 1** shows the parameters of the SPS cycle. The holding at 800°C ensured moisture evaporation, decomposition of organics, and temperature homogenization. When heating from 800 to 1350°C, the pressure increased from 17 to 60 MPa. The pressure was released from 60 to 17 MPa during the cooling stage. The sintered samples had a diameter of 20 mm and a height of around 4 mm.

Table 1. SPS cycle.

Segment Nr.	Type	Temperature, °C	Heating rate, °C/min	Duration, min	Pressure, MPa
1	Heating	RT–250	100	2.5	17
2	Heating	250–800	100	5.5	17
3	Dwell	800	0	5	17
4	Heating	800–1300	100	5	17–60
5	Heating	1300–1350	75	0.67	60
6	Dwell	1350	0	10	60
7	Cooling	1350–640	Forced cooling	5	60–17
8	Cooling	640–RT	Free cooling	75	17

2.3. Hardness and microstructure

The density of the sintered samples was measured using the Archimedes method (ISO 18754:2013). Relative densities were calculated with the theoretical density of 6.05 $g \cdot cm^{-3}$ for 3YSZ (Tosoh) and 5.57 $g \cdot cm^{-3}$ for the 3YSZ-10MWCNT composite [**23**]. The latter value was determined using the rule of mixtures. Each density experiment was performed three times and averaged (**Table 2).** Vickers hardness was measured with an FM-700 (Future-Tech, Japan) tester following ISO 14705:2016. The applied load was 9.807 N with a holding time of 12 s. The average HV_1 value was taken from five measurements. The hardness values (**Table 2**) are typical for 3YSZ

ceramics and 3YSZ-10MWCNT composite [**12**]. The microstructure was studied with a GeminiSEM 450 scanning electron microscope (Zeiss, Germany). The samples were thermally etched at 1200°C for 20 min in air to increase the visibility of grain boundaries. **Fig. S1** (Supplementary Material) compares the SEM images of the microstructure before and after thermal etching. The grain size distribution was analyzed using the ImageJ software [**27**]. ImageJ allows the measurement of the area of individual grains. **Fig. S2** shows the microstructure before and after ImageJ processing. The grain size was evaluated as the diameter of a circle with an area equivalent to the area of the grain. A series of three or four SEM images (like those presented in Fig. 3) and 1000–1300 grains were analyzed for each case study. The results were collected in an Excel file, sorted by value, and statistically processed. A volumetric concentration of 10% (2.26% by weight) of MWCNT was sufficient to demonstrate the effect of carbon nanotubes on grain growth in the zirconia matrix.

Table 2. Relative density and hardness of sintered samples.

Sample ID	Relative density	HV_1, GPa	HV_1 standard deviation, GPa
3YSZ_aggl	0.997	13.16	0.04
3YSZ_son	0.999	14.45	0.18
3YSZ-10MWCNT	0.966	7.58	0.15

3. Results and discussion

Fig. 3a and **Fig. 3b** show the microstructures of the samples sintered from the initially agglomerated 3YSZ powder (left) and the sonicated 3YSZ powder (right). Both microstructures do not reveal any traces of the former agglomerates. The 3YSZ_aggl sample has a slightly larger grain size and larger pores at junction points than the 3YSZ_son sample. As a result, the hardness of the 3YSZ_aggl sample is a little higher than that of the 3YSZ_son sample (**Table 2**). In general, the difference in microstructure for these samples is marginal. Thus, sonication has a minor influence on grain size after sintering.

Fig. S1a shows the microstructure of the sintered composite before thermal etching with agglomerates of MWCNTs. The presence of MWCNTs after SPS at 1350°C was also proven by Raman spectroscopy in our previous paper [**23**]. After the carbon burns out during thermal etching, the pores replicate the MWCNTs in the microstructure (**Fig. S1b**). **Fig. 3c** shows the 3YSZ agglomerates in the composite matrix after thermal etching. **Fig. 3d** shows the boundary between a residual 3YSZ agglomerate and the 3YSZ-10MWCNT area. The grain size in the 3YSZ-10MWCNT area is smaller than in the 3YSZ agglomerate. **Figs. 3e** and **3f** show the microstructures of a residual 3YSZ agglomerate and the 3YSZ-10MWCNT area separately and at

higher magnification. A comparison of these microstructures confirms the retarding effect of carbon nanotubes on grain growth. In summary, the MWCNTs reduce grain growth in the zirconia matrix, and powder sonication barely influences the grain size after sintering.

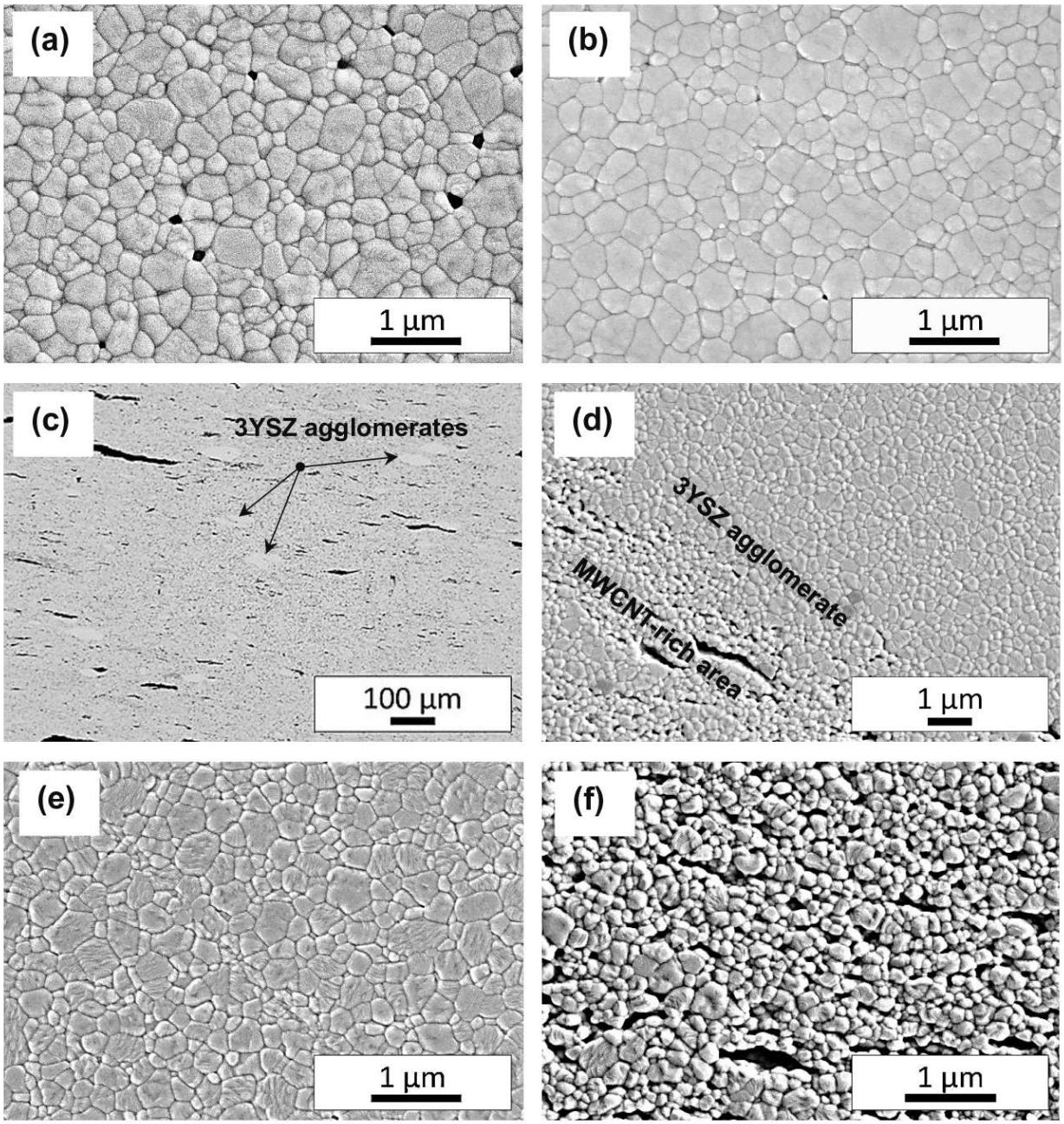

Fig. 3. Microstructure of the samples sintered from (a) initially agglomerated 3YSZ powder and (b) sonicated 3YSZ powder. (c) Microstructure of the sintered 3YSZ-10MWCNT composite with 3YSZ agglomerates. After thermal etching, the pores replicate the individual MWCNTs and MWCNT's agglomerates. (d) The boundary between the 3YSZ-10MWCNT area and the 3YSZ agglomerate. (e) Microstructure of the residual 3YSZ agglomerate. (f) Microstructure of the MWCNT-rich area in the sintered 3YSZ-10MWCNT composite.

Three mechanisms may govern the reduced grain growth in the 3YSZ-10MWCNT composite. First, the MWCNTs restrict the 3YSZ grain boundary motion because the 3YSZ/MWCNT interface is incoherent due to different atomic structures of zirconia and carbon nanotubes. The literature refers to this phenomenon as the Zener pinning effect [**29**]. Second, the individual MWCNTs and MWCNT agglomerates prevent grain fusion. Third, the CNT reaction with zirconia may form ZrO_xC_y precipitations and restrict grain growth due to the Zener effect. The fast diffusion of carbon along grain boundaries contributes to this feature [**28**]. The impact of CNTs on grain growth is moderate at 1350°C but can increase with temperature [**19**]. Detailed observation shows an inhomogeneous grain size distribution in all microstructures (**Fig. 3**). Therefore, the proper grain size characterization requires statistical analysis. The technique for doing this was adapted from the study of the particle size distribution [**30**]. **Fig. 4a** shows the cumulative grain size distributions for three sintered samples: 3YSZ_aggl, 3YSZ_son, and 3YSZ-10MWCNT. The 3YSZ-10MWCNT sample consists of two areas. The first area (3YSZ-10MWCNT_aggl) corresponds to residual zirconia agglomerates (**Fig. 3e**), and the second area (3YSZ-10MWCNT_comp) is the MWCNT-rich part of the composite (**Fig. 3f**). **Table 3** shows the percentage of grains with a size below a certain number. The median grain size D_{50} divides the distribution into two parts with equal amounts of smaller and larger grains. The value $S = (D_{90}-D_{10})/D_{50}$ characterizes the width of the distribution (ISO 9276:2014). Sonication of the 3YSZ powder leads to a slight reduction in the grain size of the sintered sample (**Fig. 4a**). The grain size of the residual 3YSZ agglomerates in the sintered composite (**Figs. 3c** and **3f**) is even smaller. The reason is the stronger boundaries between primary particles in residual 3YSZ agglomerates. The firm boundaries prevent these agglomerates from disintegrating during sonication and hinder grain fusion during sintering. The width of the grain size distribution in the 3YSZ-10MWCNT_aggl area is the same as in the 3YSZ_aggl sample. The grain size in the MWCNT-rich region is about 1.6-1.7 times smaller than in residual 3YSZ agglomerates. (**Fig. 3d**). The grain size distribution in the MWCNT-rich area is more expansive because of the retardation effect of nanotubes on grain growth and lower number of large grains. The cumulative grain area distribution in **Fig. 4b** shows a trend like the grain size distribution. Interestingly, the grain area distribution is narrower than the grain size distribution (**Table 4**).

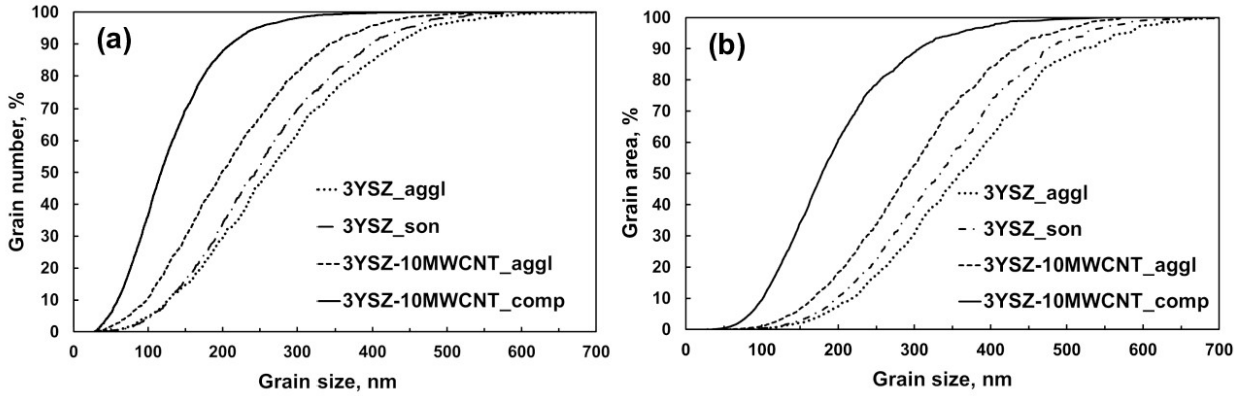

Fig. 4. Cumulative distribution of (a) grain size and (b) grain area.

Table 3. Characteristics of the grain size distribution.

Sample ID	D_{10}, μm	D_{50}, μm	D_{90}, μm	Distribution width
3YSZ_aggl	0.127	0.263	0.432	1.16
3YSZ_son	0.129	0.244	0.398	1.10
3YSZ-10MWCNT_aggl	0.098	0.199	0.342	1.23
3YSZ-10MWCNT_comp	0.059	0.117	0.211	1.30

Table 4. Characteristics of the grain area distribution.

Sample ID	S_{10}, μm^2	S_{50}, μm^2	S_{90}, μm^2	Distribution width
3YSZ_aggl	0.218	0.360	0.520	0.84
3YSZ_son	0.199	0.334	0.476	0.83
3YSZ-10MWCNT_aggl	0.167	0.293	0.435	0.91
3YSZ-10MWCNT_comp	0.101	0.178	0.306	1.15

4. Conclusions

In summary, sonication of 3YSZ powder slightly reduces grain size in sintered samples due to the disintegration of weak agglomerates. Hard agglomerates have a strong bond between primary particles. Therefore, the hard agglomerates can withstand sonication and mixing without disintegration. Firm and less movable grain boundaries in hard agglomerates result in smaller grains in residual agglomerates compared to the average grain size in the sintered 3YSZ sample. The retarding effect of carbon nanotubes on grain growth during spark plasma sintering at 1350°C is moderate. The grain size in the MWCNT-rich region is about 1.6-1.7 times smaller than in the residual 3YSZ agglomerate and 2.0-2.2 times smaller than in sintered 3YSZ samples. This effect is more pronounced when the 3YSZ-CNT composite is sintered at a higher temperature of 1700-1800°C [**18**]. The decreased grain growth results from the pinning of zirconia grain boundaries by MWCNTs due to the incoherent 3YSZ/MWCNT (Zener pinning). Additionally, individual MWCNTs and MWCNT agglomerates prevent grain fusion. Finally, the carbon and zirconia

reaction may result in oxycarbide (ZrOxCy) precipitations restricting grain growth due to the Zener effect. The statistical grain size evaluation borrowed from the particle size analysis is more informative than the common characterization by the mean grain size or a histogram. This analysis assumes the consistent processing of multiple microstructural images. The SPS sintering at 1350°C ensured full densification of 3YSZ samples with an HV_1 hardness of 13.2-14.5 GPa. The residual porosity of the 3YSZ-10MWCNT samples was approximately 3.5%, and the HV_1 hardness was 7.6 GPa. Hardness values are typical for 3YSZ ceramics and the 3YSZ-10MWCNT composite.

CRediT authorship contribution statement

Alexander M. Laptev: Conceptualization, Methodology, Data Curation, Writing – original draft. **Wiktoria Krzyżaniak:** Formal analysis, Investigation, Validation. **Maria Wiśniewska:** Visualization, Project administration. **Martin Bram:** Resources, Writing – review & editing. **Doris Sebold:** Investigation. **Dariusz Garbiec:** Supervision, Funding acquisition.

Declaration of competing interest

The authors declare that they have no known competing financial interests or personal relationships that could have appeared to influence the work reported in this paper.

Acknowledgments

The authors acknowledge the funding support from the European Commission through the Horizon 2020 - Industrial Leadership program (grant number 814632).

Appendix A. Supplementary data

Supplementary data to this article can be found online at https://doi: XXX

Data availability

Data will be made available on request.

References

[1] S.K. Soni, B. Thomas, V.R. Kar, A comprehensive review on CNTs and CNT-reinforced composites: Syntheses, characteristics and applications, Mater. Today Commun. 25 (2020) 101546. https://doi.org/10.1016/j.mtcomm.2020.101546.

[2] N. Gupta, S.M. Gupta, S.K. Sharma, Carbon nanotubes: synthesis, properties and engineering applications, Carbon Lett. 29 (2019) 419-447. https://doi.org/10.1007/s42823-019-00068-2.

[3] K. Balázsi, M. Furkó, C. Balázsi, Ceramic matrix graphene and carbon nanotube composites, in: M. Pomeroy (Ed.), Encyclopedia of Materials: Technical Ceramics and Glasses, Volume 2, Elsevier, Amsterdam, 2021, pp. 243–259. https://doi.org:/10.1016/B978-0-12-818542-1.00070-9.

[4] W.A. Curtin, B.W. Sheldon, CNT-reinforced ceramics and metals, Mater. Today 7 (2004) 44-49. https://doi.org/10.1016/S1369-7021(04)00508-5.

[5] S. Lamnini, D. Pugliese, F. Baino, Zirconia-based ceramics reinforced by carbon nanotubes: A review with emphasis on mechanical properties, Ceramics 6 (2023) 1705-1734. https://doi.org/10.3390/ceramics6030105.

[6] M. Mazaheri, D. Mari, R. Schaller, G. Bonnefont, G. Fantozzi, Processing of yttria-stabilized zirconia reinforced with multi-walled carbon nanotubes with attractive mechanical properties, J. Eur. Ceram. Soc. 31 (2011) 2691-2698. https://doi.org/10.1016/j.jeurceramsoc.2010.11.009.

[7] J.P. Zhou, Q.M. Gong, K.J. Yuan, J.J. Wu, Y.F. Chen, C.S. Li, J. Liang, The effects of multiwalled carbon nanotubes on the hot-pressed 3 mol. % yttria-stabilized zirconia ceramics, Mater. Sci. Eng. A 520 (2009) 153-157. https://doi.org/10.1016/j.msea.2009.05.014.

[8] S.L. Shi, J. Liang, Effect of multiwall carbon nanotubes on electrical and dielectric properties of yttria-stabilized zirconia ceramic, J. Am. Ceramics Soc. 89 (2006) 3533-3535. https://doi.org/10.1111/j.1551-2916.2006.01232.x.

[9] J.-H. Shin, S.-H. Hong, Microstructure and mechanical properties of single wall carbon nanotube reinforced yttria stabilized zirconia ceramics, Mater. Sci. Eng. A 556 (2012) 382-387. https://doi.org/10.1016/j.msea.2012.07.001.

[10] J. Sun, L. Gao, M. Iwasa, T. Nakayama, K. Niihara, Failure investigation of carbon nanotube/3Y-TZP nanocomposites, Ceram. Int. 31 (2005) 1131-1134. https://doi.org/10.1016/j.ceramint.2004.11.010.

[11] A. Kasperski, A. Weibel, D. Alkattan, C. Estournès, C. Laurent, A. Peigney, Double-walled carbon nanotube/zirconia composites: Preparation by spark plasma sintering, electrical conductivity and mechanical properties, Ceram. Int. 41 (2015) 13731-13738. https://doi.org/10.1016/j.ceramint.2015.08.034.

[12] L. Melk, M.L. Antti, M. Anglada, Material removal mechanisms by EDM of zirconia reinforced MWCNT nanocomposites, Ceram. Int. 42 (2016) 5792-5801. https://doi.org/10.1016/j.ceramint.2015.12.120.

[13] M. Wiśniewska, A.M. Laptev, M. Marczewski, V. Leshchynsky, G. Lota, I. Acznik, L. Celotti, A. Sullivan, M. Szybovicz, D. Garbiec, Influence of carbon nanotubes on the thermal and electrical conductivity of zirconia-based composite, Ceram. Int. 49 (2023) 15442-15450. https://doi.org/10.1016/j.ceramint.2023.01.129.

[14] A. Duszová, J. Dusza, K. Tomášek, G. Blugan, J. Kuebler, Microstructure and properties of carbon nanotube/zirconia composite. J. Eur. Ceram. Soc. 28 (2008) 1023-1027. https://doi.org/10.1016/j.jeurceramsoc.2007.09.011.

[15] A. Maitre, P. Lefort, Solid state reaction of zirconia with carbon, Solid State Ionics 104 (1997) 109-122. https://doi.org/10.1016/S0167-2738(97)00398-6.

[16] L.M. Berger, W. Gruner, E. Langholf, S. Stolle, On the mechanism of carbothermal reduction processes of TiO_2 and ZrO_2, Int. J. Refract. Metals Hard Mater. 17 (1999) 235-243. https://doi.org/10.1016/S0263-4368(98)00077-8.

[17] E. Giorgi, S. Grasso, E. Zapata-Solvas, W.E. Lee, Reactive carbothermal reduction of ZrC and ZrOC using spark plasma sintering, Adv. Appl. Ceram. 117 (2018) S34-S47. https://doi.org/10.1080/17436753.2018.1510817.

[18] B. Milsom, H. Porwal, G. Viola, Z. Gao, M.J. Reece, Understanding and quantification of grain growth mechanism in ZrO_2 carbon nanotube composites, Mater. Des. 133 (2017) 325-331. https://doi.org/10.1016/j.matdes.2017.07.040.

[19] B. Milsom, G. Viola, Z. Gao, F. Inam, T. Peijs, M.J. Reece, The effect of carbon nanotubes on the sintering behavior of zirconia, J. Eur. Ceram. Soc. 32 (2012) 4149-4156. https://doi.org/10.1016/j.jeurceramsoc.2012.07.028.

[20] A. Karanam, L. Bichler, R. Fong, On the densification behavior of (0.2, 0.5, and 1 wt. pct) CNT-YSZ ceramic composites processed via spark plasma sintering, Metall. Mater. Trans. B 46 (2015) 1666-1673. https://doi.org/10.1007/s11663-015-0317-y.

[21] F. Inam, H. Yan, T. Peijs, M.J. Reece, The sintering and grain growth behavior of ceramic–carbon nanotube nanocomposites, Compos. Sci. Technol. 70 (2010) 947-952. https://doi.org/10.1016/j.compscitech.2010.02.010.

[22] S.B. Martín, R. Poyato, D.G. García, A.D. Rodríguez, Processing of SWNT-reinforced yttria stabilized zirconia by spark plasma sintering and microstructure characterization, J. Nano Res. 18–19 (2012) 317-323. https://doi.org/10.4028/www.scientific.net/JNanoR.18-19.317.

[23] M. Wiśniewska, A.M. Laptev, M. Marczewski, W. Krzyżaniak, V. Leshchynsky, L. Celotti, M. Szybowicz, D. Garbiec, Towards homogeneous spark plasma sintering of complex-shaped ceramic matrix composites, J. Eur. Ceram. Soc. 44 (2024) 7139-7148. https://doi.org/10.1016/j.jeurceramsoc.2024.04.065.

[24] D.L. Wood, K. Nassau, Refractive index of cubic zirconia stabilized with yttria, Appl. Opt. 21 (1982) 2978-2981. https://doi.org/10.1364/AO.21.002978.

[25] A.M. Laptev, M. Bram, D. Garbiec, J. Räthel, Y. Beynet, J. Huber, M. Küster, M. Cologna, O. Guillon, Tooling in spark plasma sintering technology: Design, optimization, and application. Adv. Eng. Mater. 26, (2024) 2301391. https://doi.org/10.1002/adem.202301391.

[26] A.M. Laptev, M. Bram, K. Vanmeensel, J. Gonzalez-Juliana, O. Guillon, Enhancing the efficiency of field-assisted sintering by advanced thermal insulation, J. Mater. Process. Technol. 262 (2018) 326-339. https://doi.org/10.1016/j.jmatprotec.2018.07.008.

[27] C.A. Schneider, W.S. Rasband, K.W. Eliceiri, (2012). NIH Image to ImageJ: 25 years of image analysis, Nat. Methods 9 (2012) 671-675. https://doi.org/10.1038/nmeth.2089.

[28] A. Sondhi, C. Morandi, R.F. Reidy, T.W. Scharf, Theoretical and experimental investigations on the mechanism of carbothermal reduction of zirconia, Ceram. Int. 39 (2013) 4489-4497. http://dx.doi.org/10.1016/j.ceramint.2012.11.043.

[29] C.H. Wörner, P.M. Hazzledine, Grain growth stagnation by inclusions or pores, JOM 44 (1992) 16-20. https://doi.org/10.1007/BF03222320

[30] A. Jillavenkatesa, S.J. Dapkunas, L.S.H. Lum, Particle Size Characterization, National Institute of Standards and Technology, Gaithersburg, 2001. https://doi.org/10.6028/NBS.SP.960-1.

Supplementary Material

Impact of carbon nanotubes on grain growth during spark plasma sintering of a 3YSZ matrix composite with statistical analysis

Alexander M. Laptev [a], Wiktoria Krzyżaniak [a], Maria Wiśniewska [a], Martin Bram [b], Doris Sebold [b], Dariusz Garbiec [a]

[a] *Łukasiewicz Research Network – Poznań Institute of Technology, 6 Ewarysta Estkowskiego St., 61-755 Poznan, Poland*

[b] *Institute of Energy Materials and Devices – Materials Synthesis and Processing, Forschungszentrum Jülich GmbH, 52425 Jülich, Germany*

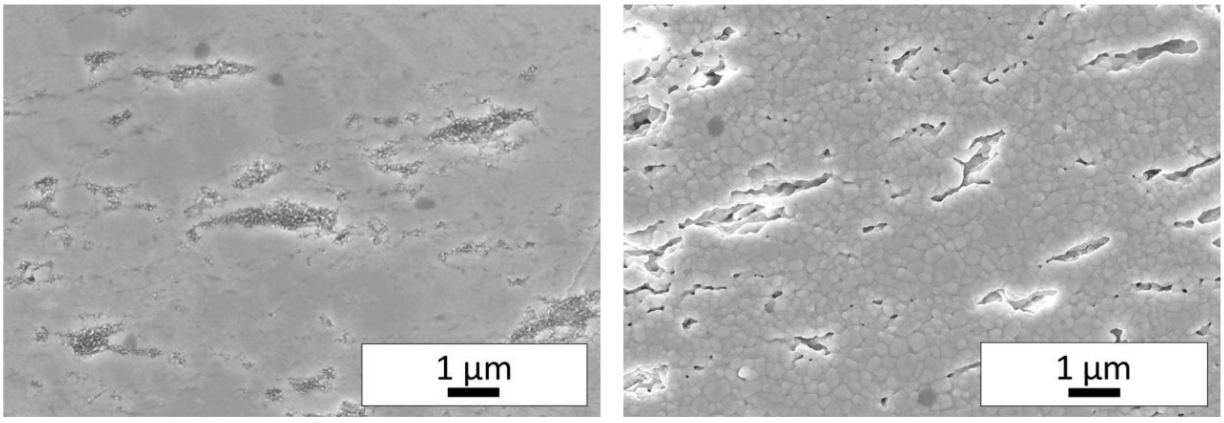

Fig. S1. Microstructure of sintered 3YSZ-10MWCNT composite **(a)** before and **(b)** after thermal etching at 1200°C for 20 min. Pores replicate the MWCNTs after their burnout during thermal etching.

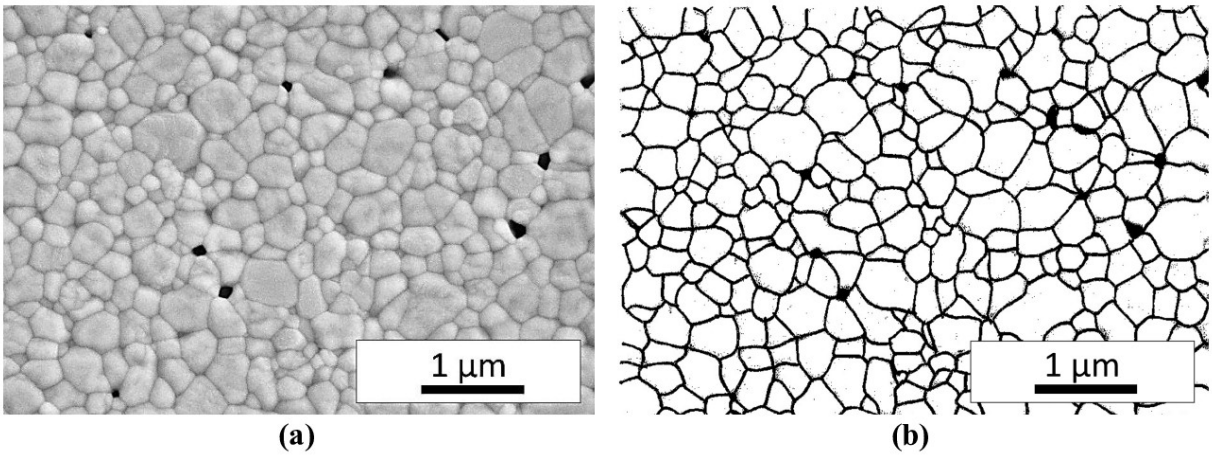

Fig. S2. (a) SEM image of 3YSZ microstructure and **(b)** the same image after processing with ImageJ software.